Search for the standard model Higgs boson in the $p\bar{p} \to ZH \to \nu\bar{\nu}b\bar{b}$ channel

V.M. Abazov, B. Abbott, M. Abolins, B.S. Acharya, M. Adams, T. Adams, M. Agelou, J.-L. Agram, S.H. Ahn, M. Ahsan, et al.

FERMILAB-PUB-06/238-E

Search for the Standard Model Higgs Boson in the $p\bar{p} \to ZH \to \nu\bar{\nu}b\bar{b}$ channel

V.M. Abazov,[36] B. Abbott,[76] M. Abolins,[66] B.S. Acharya,[29] M. Adams,[52] T. Adams,[50] M. Agelou,[18] J.-L. Agram,[19] S.H. Ahn,[31] M. Ahsan,[60] G.D. Alexeev,[36] G. Alkhazov,[40] A. Alton,[65] G. Alverson,[64] G.A. Alves,[2] M. Anastasoaie,[35] T. Andeen,[54] S. Anderson,[46] B. Andrieu,[17] M.S. Anzelc,[54] Y. Arnoud,[14] M. Arov,[53] A. Askew,[50] B. Åsman,[41] A.C.S. Assis Jesus,[3] O. Atramentov,[58] C. Autermann,[21] C. Avila,[8] C. Ay,[24] F. Badaud,[13] A. Baden,[62] L. Bagby,[53] B. Baldin,[51] D.V. Bandurin,[60] P. Banerjee,[29] S. Banerjee,[29] E. Barberis,[64] P. Bargassa,[81] P. Baringer,[59] C. Barnes,[44] J. Barreto,[2] J.F. Bartlett,[51] U. Bassler,[17] D. Bauer,[44] A. Bean,[59] M. Begalli,[3] M. Begel,[72] C. Belanger-Champagne,[5] L. Bellantoni,[51] A. Bellavance,[68] J.A. Benitez,[66] S.B. Beri,[27] G. Bernardi,[17] R. Bernhard,[42] L. Berntzon,[15] I. Bertram,[43] M. Besançon,[18] R. Beuselinck,[44] V.A. Bezzubov,[39] P.C. Bhat,[51] V. Bhatnagar,[27] M. Binder,[25] C. Biscarat,[43] K.M. Black,[63] I. Blackler,[44] G. Blazey,[53] F. Blekman,[44] S. Blessing,[50] D. Bloch,[19] K. Bloom,[68] U. Blumenschein,[23] A. Boehnlein,[51] O. Boeriu,[56] T.A. Bolton,[60] G. Borissov,[43] K. Bos,[34] T. Bose,[78] A. Brandt,[79] R. Brock,[66] G. Brooijmans,[71] A. Bross,[51] D. Brown,[79] N.J. Buchanan,[50] D. Buchholz,[54] M. Buehler,[82] V. Buescher,[23] S. Burdin,[51] S. Burke,[46] T.H. Burnett,[83] E. Busato,[17] C.P. Buszello,[44] J.M. Butler,[63] P. Calfayan,[25] S. Calvet,[15] J. Cammin,[72] S. Caron,[34] W. Carvalho,[3] B.C.K. Casey,[78] N.M. Cason,[56] H. Castilla-Valdez,[33] S. Chakrabarti,[29] D. Chakraborty,[53] K.M. Chan,[72] A. Chandra,[49] D. Chapin,[78] F. Charles,[19] E. Cheu,[46] F. Chevallier,[14] D.K. Cho,[63] S. Choi,[32] B. Choudhary,[28] L. Christofek,[59] D. Claes,[68] B. Clément,[19] C. Clément,[41] Y. Coadou,[5] M. Cooke,[81] W.E. Cooper,[51] D. Coppage,[59] M. Corcoran,[81] M.-C. Cousinou,[15] B. Cox,[45] S. Crépé-Renaudin,[14] D. Cutts,[78] M. Ćwiok,[30] H. da Motta,[2] A. Das,[63] M. Das,[61] B. Davies,[43] G. Davies,[44] G.A. Davis,[54] K. De,[79] P. de Jong,[34] S.J. de Jong,[35] E. De La Cruz-Burelo,[65] C. De Oliveira Martins,[3] J.D. Degenhardt,[65] F. Déliot,[18] M. Demarteau,[51] R. Demina,[72] P. Demine,[18] D. Denisov,[51] S.P. Denisov,[39] S. Desai,[73] H.T. Diehl,[51] M. Diesburg,[51] M. Doidge,[43] A. Dominguez,[68] H. Dong,[73] L.V. Dudko,[38] L. Duflot,[16] S.R. Dugad,[29] A. Duperrin,[15] J. Dyer,[66] A. Dyshkant,[53] M. Eads,[68] D. Edmunds,[66] T. Edwards,[45] J. Ellison,[49] J. Elmsheuser,[25] V.D. Elvira,[51] S. Eno,[62] P. Ermolov,[38] J. Estrada,[51] H. Evans,[55] A. Evdokimov,[37] V.N. Evdokimov,[39] S.N. Fatakia,[63] L. Feligioni,[63] A.V. Ferapontov,[60] T. Ferbel,[72] F. Fiedler,[25] F. Filthaut,[35] W. Fisher,[51] H.E. Fisk,[51] I. Fleck,[23] M. Ford,[45] M. Fortner,[53] H. Fox,[23] S. Fu,[51] S. Fuess,[51] T. Gadfort,[83] C.F. Galea,[35] E. Gallas,[51] E. Galyaev,[56] C. Garcia,[72] A. Garcia-Bellido,[83] J. Gardner,[59] V. Gavrilov,[37] A. Gay,[19] P. Gay,[13] D. Gelé,[19] R. Gelhaus,[49] C.E. Gerber,[52] Y. Gershtein,[50] D. Gillberg,[5] G. Ginther,[72] N. Gollub,[41] B. Gómez,[8] A. Goussiou,[56] P.D. Grannis,[73] H. Greenlee,[51] Z.D. Greenwood,[61] E.M. Gregores,[4] G. Grenier,[20] Ph. Gris,[13] J.-F. Grivaz,[16] S. Grünendahl,[51] M.W. Grünewald,[30] F. Guo,[73] J. Guo,[73] G. Gutierrez,[51] P. Gutierrez,[76] A. Haas,[71] N.J. Hadley,[62] P. Haefner,[25] S. Hagopian,[50] J. Haley,[69] I. Hall,[76] R.E. Hall,[48] L. Han,[7] K. Hanagaki,[51] K. Harder,[60] A. Harel,[72] R. Harrington,[64] J.M. Hauptman,[58] R. Hauser,[66] J. Hays,[54] T. Hebbeker,[21] D. Hedin,[53] J.G. Hegeman,[34] J.M. Heinmiller,[52] A.P. Heinson,[49] U. Heintz,[63] C. Hensel,[59] G. Hesketh,[64] M.D. Hildreth,[56] R. Hirosky,[82] J.D. Hobbs,[73] B. Hoeneisen,[12] H. Hoeth,[26] M. Hohlfeld,[16] S.J. Hong,[31] R. Hooper,[78] P. Houben,[34] Y. Hu,[73] Z. Hubacek,[10] V. Hynek,[9] I. Iashvili,[70] R. Illingworth,[51] A.S. Ito,[51] S. Jabeen,[63] M. Jaffré,[16] S. Jain,[76] K. Jakobs,[23] C. Jarvis,[62] A. Jenkins,[44] R. Jesik,[44] K. Johns,[46] C. Johnson,[71] M. Johnson,[51] A. Jonckheere,[51] P. Jonsson,[44] A. Juste,[51] D. Käfer,[21] S. Kahn,[74] E. Kajfasz,[15] A.M. Kalinin,[36] J.M. Kalk,[61] J.R. Kalk,[66] S. Kappler,[21] D. Karmanov,[38] J. Kasper,[63] P. Kasper,[51] I. Katsanos,[71] D. Kau,[50] R. Kaur,[27] R. Kehoe,[80] S. Kermiche,[15] S. Kesisoglou,[78] N. Khalatyan,[63] A. Khanov,[77] A. Kharchilava,[70] Y.M. Kharzheev,[36] D. Khatidze,[71] H. Kim,[79] T.J. Kim,[31] M.H. Kirby,[35] B. Klima,[51] J.M. Kohli,[27] J.-P. Konrath,[23] M. Kopal,[76] V.M. Korablev,[39] J. Kotcher,[74] B. Kothari,[71] A. Koubarovsky,[38] A.V. Kozelov,[39] J. Kozminski,[66] D. Krop,[55] A. Kryemadhi,[82] T. Kuhl,[24] A. Kumar,[70] S. Kunori,[62] A. Kupco,[11] T. Kurča,[20,*] J. Kvita,[9] S. Lager,[41] S. Lammers,[71] G. Landsberg,[78] J. Lazoflores,[50] A.-C. Le Bihan,[19] P. Lebrun,[20] W.M. Lee,[53] A. Leflat,[38] F. Lehner,[42] V. Lesne,[13] J. Leveque,[46] P. Lewis,[44] J. Li,[79] Q.Z. Li,[51] J.G.R. Lima,[53] D. Lincoln,[51] J. Linnemann,[66] V.V. Lipaev,[39] R. Lipton,[51] Z. Liu,[5] L. Lobo,[44] A. Lobodenko,[40] M. Lokajicek,[11] A. Lounis,[19] P. Love,[43] H.J. Lubatti,[83] M. Lynker,[56] A.L. Lyon,[51] A.K.A. Maciel,[2] R.J. Madaras,[47] P. Mättig,[26] C. Magass,[21] A. Magerkurth,[65] A.-M. Magnan,[14] N. Makovec,[16] P.K. Mal,[56] H.B. Malbouisson,[3] S. Malik,[68] V.L. Malyshev,[36] H.S. Mao,[6] Y. Maravin,[60] M. Martens,[51] S.E.K. Mattingly,[78] R. McCarthy,[73] D. Meder,[24] A. Melnitchouk,[67] A. Mendes,[15] L. Mendoza,[8] M. Merkin,[38] K.W. Merritt,[51] A. Meyer,[21] J. Meyer,[22] M. Michaut,[18] H. Miettinen,[81] T. Millet,[20] J. Mitrevski,[71] J. Molina,[3] N.K. Mondal,[29]

J. Monk,[45] R.W. Moore,[5] T. Moulik,[59] G.S. Muanza,[16] M. Mulders,[51] M. Mulhearn,[71] L. Mundim,[3] Y.D. Mutaf,[73] E. Nagy,[15] M. Naimuddin,[28] M. Narain,[63] N.A. Naumann,[35] H.A. Neal,[65] J.P. Negret,[8] S. Nelson,[50] P. Neustroev,[40] C. Noeding,[23] A. Nomerotski,[51] S.F. Novaes,[4] T. Nunnemann,[25] V. O'Dell,[51] D.C. O'Neil,[5] G. Obrant,[40] V. Oguri,[3] N. Oliveira,[3] N. Oshima,[51] R. Otec,[10] G.J. Otero y Garzón,[52] M. Owen,[45] P. Padley,[81] N. Parashar,[57] S.-J. Park,[72] S.K. Park,[31] J. Parsons,[71] R. Partridge,[78] N. Parua,[73] A. Patwa,[74] G. Pawloski,[81] P.M. Perea,[49] E. Perez,[18] K. Peters,[45] P. Pétroff,[16] M. Petteni,[44] R. Piegaia,[1] M.-A. Pleier,[22] P.L.M. Podesta-Lerma,[33] V.M. Podstavkov,[51] Y. Pogorelov,[56] M.-E. Pol,[2] A. Pomposš,[76] B.G. Pope,[66] A.V. Popov,[39] W.L. Prado da Silva,[3] H.B. Prosper,[50] S. Protopopescu,[74] J. Qian,[65] A. Quadt,[22] B. Quinn,[67] K.J. Rani,[29] K. Ranjan,[28] P.N. Ratoff,[43] P. Renkel,[80] S. Reucroft,[64] M. Rijssenbeek,[73] I. Ripp-Baudot,[19] F. Rizatdinova,[77] S. Robinson,[44] R.F. Rodrigues,[3] C. Royon,[18] P. Rubinov,[51] R. Ruchti,[56] V.I. Rud,[38] G. Sajot,[14] A. Sánchez-Hernández,[33] M.P. Sanders,[62] A. Santoro,[3] G. Savage,[51] L. Sawyer,[61] T. Scanlon,[44] D. Schaile,[25] R.D. Schamberger,[73] Y. Scheglov,[40] H. Schellman,[54] P. Schieferdecker,[25] C. Schmitt,[26] C. Schwanenberger,[45] A. Schwartzman,[69] R. Schwienhorst,[66] S. Sengupta,[50] H. Severini,[76] E. Shabalina,[52] M. Shamim,[60] V. Shary,[18] A.A. Shchukin,[39] W.D. Shephard,[56] R.K. Shivpuri,[28] D. Shpakov,[51] V. Siccardi,[19] R.A. Sidwell,[60] V. Simak,[10] V. Sirotenko,[51] P. Skubic,[76] P. Slattery,[72] R.P. Smith,[51] G.R. Snow,[68] J. Snow,[75] S. Snyder,[74] S. Söldner-Rembold,[45] X. Song,[53] L. Sonnenschein,[17] A. Sopczak,[43] M. Sosebee,[79] K. Soustruznik,[9] M. Souza,[2] B. Spurlock,[79] J. Stark,[14] J. Steele,[61] V. Stolin,[37] A. Stone,[52] D.A. Stoyanova,[39] J. Strandberg,[41] M.A. Strang,[70] M. Strauss,[76] R. Ströhmer,[25] D. Strom,[54] M. Strovink,[47] L. Stutte,[51] S. Sumowidagdo,[50] A. Sznajder,[3] M. Talby,[15] P. Tamburello,[46] W. Taylor,[5] P. Telford,[45] J. Temple,[46] B. Tiller,[25] M. Titov,[23] V.V. Tokmenin,[36] M. Tomoto,[51] T. Toole,[62] I. Torchiani,[23] S. Towers,[43] T. Trefzger,[24] S. Trincaz-Duvoid,[17] D. Tsybychev,[73] B. Tuchming,[18] C. Tully,[69] A.S. Turcot,[45] P.M. Tuts,[71] R. Unalan,[66] L. Uvarov,[40] S. Uvarov,[40] S. Uzunyan,[53] B. Vachon,[5] P.J. van den Berg,[34] R. Van Kooten,[55] W.M. van Leeuwen,[34] N. Varelas,[52] E.W. Varnes,[46] A. Vartapetian,[79] I.A. Vasilyev,[39] M. Vaupel,[26] P. Verdier,[20] L.S. Vertogradov,[36] M. Verzocchi,[51] F. Villeneuve-Seguier,[44] P. Vint,[44] J.-R. Vlimant,[17] E. Von Toerne,[60] M. Voutilainen,[68,†] M. Vreeswijk,[34] H.D. Wahl,[50] L. Wang,[62] J. Warchol,[56] G. Watts,[83] M. Wayne,[56] M. Weber,[51] H. Weerts,[66] N. Wermes,[22] M. Wetstein,[62] A. White,[79] D. Wicke,[26] G.W. Wilson,[59] S.J. Wimpenny,[49] M. Wobisch,[51] J. Womersley,[51] D.R. Wood,[64] T.R. Wyatt,[45] Y. Xie,[78] N. Xuan,[56] S. Yacoob,[54] R. Yamada,[51] M. Yan,[62] T. Yasuda,[51] Y.A. Yatsunenko,[36] K. Yip,[74] H.D. Yoo,[78] S.W. Youn,[54] C. Yu,[14] J. Yu,[79] A. Yurkewicz,[73] A. Zatserklyaniy,[53] C. Zeitnitz,[26] D. Zhang,[51] T. Zhao,[83] B. Zhou,[65] J. Zhu,[73] M. Zielinski,[72] D. Zieminska,[55] A. Zieminski,[55] V. Zutshi,[53] and E.G. Zverev[38]

(DØ Collaboration)

[1] *Universidad de Buenos Aires, Buenos Aires, Argentina*
[2] *LAFEX, Centro Brasileiro de Pesquisas Físicas, Rio de Janeiro, Brazil*
[3] *Universidade do Estado do Rio de Janeiro, Rio de Janeiro, Brazil*
[4] *Instituto de Física Teórica, Universidade Estadual Paulista, São Paulo, Brazil*
[5] *University of Alberta, Edmonton, Alberta, Canada, Simon Fraser University, Burnaby, British Columbia, Canada, York University, Toronto, Ontario, Canada, and McGill University, Montreal, Quebec, Canada*
[6] *Institute of High Energy Physics, Beijing, People's Republic of China*
[7] *University of Science and Technology of China, Hefei, People's Republic of China*
[8] *Universidad de los Andes, Bogotá, Colombia*
[9] *Center for Particle Physics, Charles University, Prague, Czech Republic*
[10] *Czech Technical University, Prague, Czech Republic*
[11] *Center for Particle Physics, Institute of Physics, Academy of Sciences of the Czech Republic, Prague, Czech Republic*
[12] *Universidad San Francisco de Quito, Quito, Ecuador*
[13] *Laboratoire de Physique Corpusculaire, IN2P3-CNRS, Université Blaise Pascal, Clermont-Ferrand, France*
[14] *Laboratoire de Physique Subatomique et de Cosmologie, IN2P3-CNRS, Universite de Grenoble 1, Grenoble, France*
[15] *CPPM, IN2P3-CNRS, Université de la Méditerranée, Marseille, France*
[16] *IN2P3-CNRS, Laboratoire de l'Accélérateur Linéaire, Orsay, France*
[17] *LPNHE, IN2P3-CNRS, Universités Paris VI and VII, Paris, France*
[18] *DAPNIA/Service de Physique des Particules, CEA, Saclay, France*
[19] *IPHC, IN2P3-CNRS, Université Louis Pasteur, Strasbourg, France, and Université de Haute Alsace, Mulhouse, France*
[20] *Institut de Physique Nucléaire de Lyon, IN2P3-CNRS, Université Claude Bernard, Villeurbanne, France*
[21] *III. Physikalisches Institut A, RWTH Aachen, Aachen, Germany*
[22] *Physikalisches Institut, Universität Bonn, Bonn, Germany*
[23] *Physikalisches Institut, Universität Freiburg, Freiburg, Germany*
[24] *Institut für Physik, Universität Mainz, Mainz, Germany*
[25] *Ludwig-Maximilians-Universität München, München, Germany*
[26] *Fachbereich Physik, University of Wuppertal, Wuppertal, Germany*

[27] *Panjab University, Chandigarh, India*
[28] *Delhi University, Delhi, India*
[29] *Tata Institute of Fundamental Research, Mumbai, India*
[30] *University College Dublin, Dublin, Ireland*
[31] *Korea Detector Laboratory, Korea University, Seoul, Korea*
[32] *SungKyunKwan University, Suwon, Korea*
[33] *CINVESTAV, Mexico City, Mexico*
[34] *FOM-Institute NIKHEF and University of Amsterdam/NIKHEF, Amsterdam, The Netherlands*
[35] *Radboud University Nijmegen/NIKHEF, Nijmegen, The Netherlands*
[36] *Joint Institute for Nuclear Research, Dubna, Russia*
[37] *Institute for Theoretical and Experimental Physics, Moscow, Russia*
[38] *Moscow State University, Moscow, Russia*
[39] *Institute for High Energy Physics, Protvino, Russia*
[40] *Petersburg Nuclear Physics Institute, St. Petersburg, Russia*
[41] *Lund University, Lund, Sweden, Royal Institute of Technology and Stockholm University, Stockholm, Sweden, and Uppsala University, Uppsala, Sweden*
[42] *Physik Institut der Universität Zürich, Zürich, Switzerland*
[43] *Lancaster University, Lancaster, United Kingdom*
[44] *Imperial College, London, United Kingdom*
[45] *University of Manchester, Manchester, United Kingdom*
[46] *University of Arizona, Tucson, Arizona 85721, USA*
[47] *Lawrence Berkeley National Laboratory and University of California, Berkeley, California 94720, USA*
[48] *California State University, Fresno, California 93740, USA*
[49] *University of California, Riverside, California 92521, USA*
[50] *Florida State University, Tallahassee, Florida 32306, USA*
[51] *Fermi National Accelerator Laboratory, Batavia, Illinois 60510, USA*
[52] *University of Illinois at Chicago, Chicago, Illinois 60607, USA*
[53] *Northern Illinois University, DeKalb, Illinois 60115, USA*
[54] *Northwestern University, Evanston, Illinois 60208, USA*
[55] *Indiana University, Bloomington, Indiana 47405, USA*
[56] *University of Notre Dame, Notre Dame, Indiana 46556, USA*
[57] *Purdue University Calumet, Hammond, Indiana 46323, USA*
[58] *Iowa State University, Ames, Iowa 50011, USA*
[59] *University of Kansas, Lawrence, Kansas 66045, USA*
[60] *Kansas State University, Manhattan, Kansas 66506, USA*
[61] *Louisiana Tech University, Ruston, Louisiana 71272, USA*
[62] *University of Maryland, College Park, Maryland 20742, USA*
[63] *Boston University, Boston, Massachusetts 02215, USA*
[64] *Northeastern University, Boston, Massachusetts 02115, USA*
[65] *University of Michigan, Ann Arbor, Michigan 48109, USA*
[66] *Michigan State University, East Lansing, Michigan 48824, USA*
[67] *University of Mississippi, University, Mississippi 38677, USA*
[68] *University of Nebraska, Lincoln, Nebraska 68588, USA*
[69] *Princeton University, Princeton, New Jersey 08544, USA*
[70] *State University of New York, Buffalo, New York 14260, USA*
[71] *Columbia University, New York, New York 10027, USA*
[72] *University of Rochester, Rochester, New York 14627, USA*
[73] *State University of New York, Stony Brook, New York 11794, USA*
[74] *Brookhaven National Laboratory, Upton, New York 11973, USA*
[75] *Langston University, Langston, Oklahoma 73050, USA*
[76] *University of Oklahoma, Norman, Oklahoma 73019, USA*
[77] *Oklahoma State University, Stillwater, Oklahoma 74078, USA*
[78] *Brown University, Providence, Rhode Island 02912, USA*
[79] *University of Texas, Arlington, Texas 76019, USA*
[80] *Southern Methodist University, Dallas, Texas 75275, USA*
[81] *Rice University, Houston, Texas 77005, USA*
[82] *University of Virginia, Charlottesville, Virginia 22901, USA*
[83] *University of Washington, Seattle, Washington 98195, USA*

(Dated: July 13^{th}, 2006)

We report a search for the standard model (SM) Higgs boson based on data collected by the DØ experiment at the Fermilab Tevatron Collider, corresponding to an integrated luminosity of 260 pb^{-1}. We study events with missing transverse energy and two acoplanar b-jets, which provide

sensitivity to the ZH production cross section in the $\nu\bar{\nu}b\bar{b}$ channel and to WH production, when the lepton from the $W \to \ell\nu$ decay is undetected. The data are consistent with the SM background expectation, and we set 95% C.L. upper limits on $\sigma(p\bar{p} \to ZH/WH) \times B(H \to b\bar{b})$ from 3.4/8.3 to 2.5/6.3 pb, for Higgs masses between 105 and 135 GeV.

PACS numbers: 13.85.Qk, 13.85.Ni, 13.85.Rm

In the standard model (SM) the Higgs boson (H) is responsible for electroweak symmetry breaking and has not yet been observed. The experiments at the CERN e^+e^- Collider (LEP) provide lower limits on its mass, $m_H > 114.4$ GeV, while electroweak global fits favor a light Higgs boson, $m_H < 207$ GeV at 95% C.L. [1]. If it exists, the Higgs boson could be observed at the Fermilab Tevatron Collider (center of mass energy $\sqrt{s}$ =1.96 TeV) by combining different analysis channels from both the DØ and CDF experiments [2, 3].

We present a search for a SM Higgs boson with m_H between 105 and 135 GeV, in the final state with missing transverse energy ($\not\!\!E_T$) and two or three jets, in which one or two jets are identified ("tagged") as b jets. This final state is sensitive to Higgs bosons produced in the $p\bar{p} \to ZH \to \nu\bar{\nu}b\bar{b}$ channel, which is particularly promising because of the expected large $Z \to \nu\bar{\nu}$ and $H \to b\bar{b}$ branching fractions. The product of cross section (σ) and branching fraction (B) is predicted to be about 0.01 pb for a 115 GeV Higgs boson, which is comparable to that for $WH \to l\nu b\bar{b}$ [4].

The chosen final state also has sensitivity to WH production since the charged lepton from W decay can be undetected or not identified properly ($\not\!\!\ell\nu b\bar{b}$ channel). Searches for WH production have been performed previously by relying on the identification of the electron or the muon from leptonic W decay [5, 6].

There are two main sources of background to this final state: i) the "physics" backgrounds Z+jets, W+jets, electroweak diboson production (WZ and ZZ), and top quark production with undetected leptons or jets, and ii) a large instrumental background caused by multijet events with mismeasured jet energies that is difficult to simulate. In the ZH or WH processes, since the two b jets are boosted along the Higgs-momentum direction, they are not back-to-back in azimuthal angle (φ), in contrast to the dominant dijet background. Our search is based on an integrated luminosity of 260 pb^{-1} accumulated with a dedicated trigger designed to select events with significant $\not\!\!E_T$and with jets that are not back-to-back.

The DØ tracking system, consists of a silicon microstrip tracker (SMT) and a central fiber tracker (CFT), both located within a 2 T superconducting solenoidal magnet [7], with tracking and vertexing at pseudorapidities $|\eta| < 3$ and $|\eta| < 2.5$, respectively, where $\eta = -\ln(\tan(\theta/2))$, and θ is the polar angle. A liquid-argon and uranium calorimeter has a central section (CC) covering $|\eta|$ up to ≈ 1.1, and two end calorimeters (EC) that extend coverage to $|\eta| \approx 4.2$ [8]. An outer muon system, at $|\eta| < 2$, consists of a layer of tracking detectors and scintillation trigger counters in front of 1.8 T toroids, followed by two similar layers after the toroids.

To estimate the number of expected events, the signal (ZH, WH), $t\bar{t}$, and diboson production is simulated with PYTHIA [9]. For W and Z events with two or more jets we use ALPGEN [10], and for single top simulation we use COMPHEP [11]. The samples generated by COMPHEP and ALPGEN are passed through PYTHIA for showering and hadronization. The cross section for the ALPGEN samples are normalized to next-to-leading-order calculations [12]. All the samples are processed through DØ detector simulation based on GEANT [13], and DØ reconstruction software. Trigger efficiencies measured in data are applied to correct the simulated events.

Event selection requires two or three jets reconsructed with the "iterative-midpoint-Run-II" cone algorithm, with $p_T > 20$ GeV, $|\eta| < 2.5$ and a cone radius of $\Delta R = \sqrt{(\Delta\eta)^2 + (\Delta\varphi)^2} < 0.5$. Jets are required to pass quality criteria designed to reject noise and suppress electron- or photon-induced energy depositions, and jet energies are corrected to the particle level using jet energy calibration and resolution factors determined from photon+jet events. Corrections depend on the p_T and η of the jet and are typically 30%. Jet energy resolution varies from 20% to 10% for p_T between 40 and 150 GeV.

The primary vertex has to be within $\pm$35 cm in the z direction, and at least two "taggable" jets passing the above requirements must be present in the event to be included in our final sample. A jet is taggable if it contains within its cone at least two tracks satisfying strict quality criteria, one with $p_T > 1$ GeV, and another with $p_T > 0.5$ GeV. The average fraction of taggable jets is measured using $W(\to \mu\nu)$+jets data, and is (86$\pm$1)% per jet. This fraction, which is a function of η and p_T of the jet, and of the z coordinate of the primary vertex, is used to correct the simulated jets.

We then require: i) $\not\!\!E_T >$ 50 GeV, where $\not\!\!E_T$ is calculated from the position and energy of the calorimeter cells, ii) the azimuthal angle between the two highest p_T (leading) jets to be less than 165°, and iii) no isolated electrons or muons, in order to suppress multijet background and $W(\to e\nu, \mu\nu)$+jet, and $Z(\to ee, \mu\mu)$+jet events. For the rejection of $t\bar{t}$ background, we require the scalar sum H_T of the p_T of the jets to be less than 240 GeV. To further reduce instrumental background induced by mismeasurement of jet energy, which produces abnormal $\not\!\!E_T$, we define $min\Delta\varphi(\vec{\not\!\!E}_T$, jets) as the min-

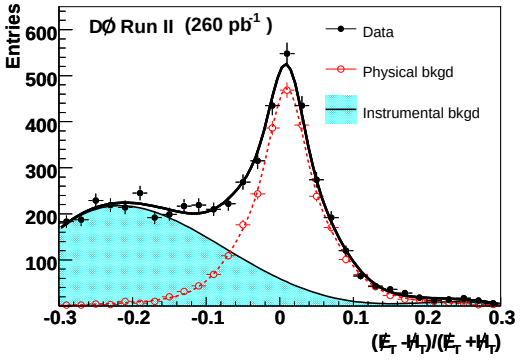

FIG. 1: Asymmetry distribution A($\not\!\!E_T$, $\not\!\!H_T$) in the signal region, prior to the imposition of the requirement on A($\not\!\!E_T$, $\not\!\!H_T$). The data is described by the sum of the physics background, modeled by a triple Gaussian, and the instrumental background modeled by a polynomial function.

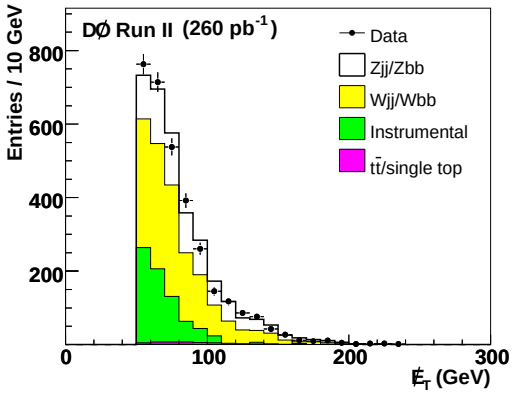

FIG. 2: $\not\!\!E_T$ distribution after selection except for b-tagging.

imum difference in φ between the direction of $\vec{\not\!\!E}_T$ and any of the jets, $\not\!\!H_T \equiv |\sum_{i=1}^{njet} \vec{p}_T|$ as the magnitude of the vector sum of the $\vec{p}_T$ of the jets, $\vec{P}_T^{trk} \equiv -\sum_{i=1}^{ntrk} \vec{p}_T$ as opposite vector sum of the $\vec{p}_T$ of all tracks, $\Delta\varphi(\vec{\not\!\!E}_T, \vec{P}_T^{trk})$ as the difference in φ between the direction of $\vec{\not\!\!E}_T$ and $\vec{P}_T^{trk}$, and A($\not\!\!E_T$, $\not\!\!H_T$)$\equiv$($\not\!\!E_T$ $-$ $\not\!\!H_T$)/($\not\!\!E_T$ $+$ $\not\!\!H_T$) as the asymmetry between $\not\!\!E_T$ and $\not\!\!H_T$. The instrumental background is significantly reduced by requiring: $\not\!\!E_T$ (in GeV) $> 80 - 40 \times min\Delta\varphi(\vec{\not\!\!E}_T, \text{jet})$, $|\vec{P}_T^{trk}| > 20$ GeV, $\Delta\varphi(\vec{\not\!\!E}_T, \vec{P}_T^{trk}) < \frac{\pi}{2}$ and $-0.1 <$ A($\not\!\!E_T$, $\not\!\!H_T$) < 0.2. All these requirements define the signal region.

$W(\rightarrow \mu\nu)$+jets data are used to confirm that the above variables are well modeled. The instrumental background is then estimated from the data using the signal and a "sideband" region, which is defined by requiring all above selections, except for the requirement $\Delta\varphi(\vec{\not\!\!E}_T, \vec{P}_T^{trk}) > \frac{\pi}{2}$. The distribution in the simulated instrumental background generated by PYTHIA gives a qualitative description of this background. This indicates that we are correctly identifying the background source, and we therefore model it using sideband data to avoid uncertainty from the difficult simulation of instrumental background. The physics backgrounds passing the final selection tend to be distributed around $\Delta\varphi(\vec{\not\!\!E}_T, \vec{P}_T^{trk}) \sim 0$, while the instrumental background is distributed similarly in the sideband and in the signal region due to mismeasurement of jet energy or of charged tracks.

Figure 1 shows the $A(\not\!\!E_T, \not\!\!H_T)$ distribution in the signal region. The amount of physics background in the signal region is estimated using the simulation, and parameterized by a triple Gaussian (TG) function, shown as a dashed line in Fig. 1. The contribution not described by this parameterization is considered to be the instrumental background, and is modeled with a polynomial function tested with a fit to the data in the sideband region. The physics background contributes about 15% of the events in the sideband region and is included in the model of instrumental background. The sum of the absolutely normalized TG parameterization and of the polynomial function is then fitted to the data in the signal region, as shown in Fig. 1. (Before b-tagging, the Higgs signal is negligible.) The instrumental background in the signal region amounts to 696$\pm$91 events, while the physics background amounts to 2520$\pm$330 events. Since our search requires good modeling of $\not\!\!E_T$, we show in Fig. 2 the $\not\!\!E_T$ distribution after all requirements, excepting b-tagging. The data are well described by the sum of the simulation of $Z/W + jj/b\bar{b}$ and the estimated contribution from instrumental background. Top pair and single top pair production represent negligible contributions before requiring b-tagging.

To select b jets, we apply a b-tagging algorithm that uses a jet lifetime probability (JLIP) computed from the tracks associated with the jet. A small probability corresponds to jets having tracks with a large impact parameter that characterize b-hadron decay. We use two samples for our search: one that requires the two leading jets to pass the b-tagging condition (double b-tagged sample, or DT sample); the other requires exactly one jet to pass the b-tagging condition, and does not accept events from the DT sample (exclusive single b-tagged sample, or ST sample). The requirements on the lifetime probability are defined by optimizing the sensitivity to Higgs signal. In the DT sample, we require JLIP $< 1\%$ for the leading jet and < 4 % for the second-leading jet. In the ST sample we require a more stringent JLIP < 0.1 %. The average b-tagging efficiency is $\approx 50\%$ (40%, 30%) for JLIP $< 4\%(1\%, 0.1\%)$. The relative uncertainty on the b-tagging efficiency is 7% per jet. The mis-tag rate is defined as the fraction of light-quark jets tagged as b jets, and its average value is approximately the value of the JLIP requirement. For the instrumental background, we estimate the mis-tag rate from data in the sideband

TABLE I: Number of expected signal (for $m_H = 115$ GeV), background, and observed events (obs.) before b-tagging, after inclusive (IST), and exclusive (ST) single b-tagging, and after double b-tagging (DT). Before b-tagging, the expected background is by construction equal to the observed events (see text on the background determination). The numbers of events after the ± 1.5 standard deviation (s.d.) mass window requirement are given in parenthesis. The errors on these numbers are in average 18% (19%) for the ST (DT) sample.

	$\not\!\!E_T$ + 2, 3 jets	$\not\!\!E_T$ + 2, 3 jets IST	$\not\!\!E_T$ + 2, 3 jets ST	$\not\!\!E_T$ + 2, 3 jets DT
ZH	0.71	0.62	0.26 (0.20)	0.24 (0.21)
WH	0.54	0.47	0.20 (0.15)	0.18 (0.15)
Zjj	843	93.3	7.9 (2.6)	1.4 (0.5)
Wjj	1600	260	36.1 (13.6)	4.2 (1.5)
Zbb	13.1	11.3	4.7 (1.6)	4.1 (1.4)
Wbb	12.4	10.5	4.4 (1.4)	3.6 (1.1)
$t\bar{t}/tb/tqb$	42.3	33.6	15.3 (5.6)	9.0 (3.0)
WZ/ZZ	7.3	3.4	1.1 (0.71)	0.9 (0.6)
Instrumental	696	143	25.0 (8.4)	3.9 (1.3)
Total expectation	$\equiv$ obs.	555	94.5 (34.0)	27.0 (9.4)
Observed events	3210	592	106 (33)	25 (11)

region, and extrapolate it into the signal region. Table I lists the number of ZH and WH signal, background and observed events for each b-tag requirement, and also for the inclusive sample of events with at least one b-tagged jet with JLIP $< 4\%$ (to verify that the data are also well described by the simulation in another b-tagging configuration). After the ST requirement, 106 events remain, while 94.5 ± 17.0 events are expected. In the DT sample, we observe 25 events, while 27.0 ± 5.1 are expected, and in the inclusive sample these numbers are 592 and 555 ± 70 events, respectively.

We estimate the systematic uncertainty due to trigger and jet reconstruction efficiency, jet energy calibration, jet resolution, b-tagging, instrumental-background estimation, physics-background cross sections and parton distribution functions, by varying each source of uncertainty by ± 1 s.d. and repeating the analysis. The systematic uncertainties are estimated separately for the DT and ST samples. In total, we find a 19% (14%) uncertainty on signal acceptance and 19% (18%) uncertainty on the total background for the DT (ST) analysis. The dominant systematic uncertainties are due to b-tagging and jet reconstruction and calibration. The uncertainty on the integrated luminosity is 6.5%.

We then search for an excess of events as a function of m_H by counting events in the dijet mass distribution within a ± 1.5 s.d. window around the reconstructed Higgs-boson mass peak, e.g., ± 25.2 GeV for m_H=115 GeV. No excess over the SM background is found in the data, as can be seen for the DT dijet mass distribution in Fig. 3, in which the expected ZH signal for $m_H = 115$ GeV is also shown. The acceptance for ZH (WH) events

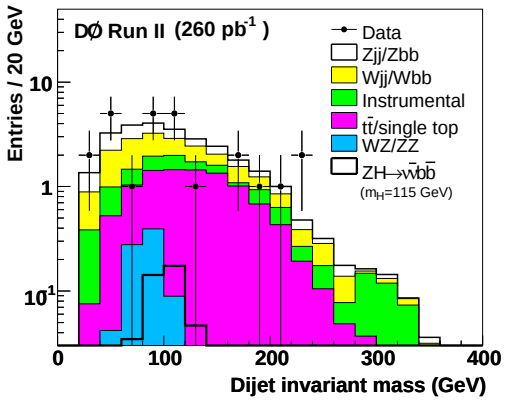

FIG. 3: Dijet invariant mass distribution in the DT sample. The expectation originating from ZH production with $m_H = 115$ GeV is also shown.

is 1.04% (0.43%) for $m_H = 115$ GeV. We thus set 95% C.L. upper limits on $\sigma(p\bar{p} \to ZH) \times B(H \to b\bar{b})$ and $\sigma(p\bar{p} \to WH) \times B(H \to b\bar{b})$, using a modified frequentist approach, the CL_S method [14]. In this method, the binned distributions are summed over the log-likelihood ratio test statistic. Systematic uncertainties are incorporated into the signal and background expectations using Gaussian sampling of individual uncertainties. For the limits obtained when combining the likelihoods of the ST and DT analyses, correlations between uncertainties are handled by varying simultaneously all identical sources. Limits are determined by scaling the signal expectations until the probability for the background-only hypothesis falls below 5% (95% C.L.). This translates into a cross-section limit for $\sigma(p\bar{p} \to ZH) \times B(H \to b\bar{b})$ of 3.2 pb and for $\sigma(p\bar{p} \to WH) \times B(H \to b\bar{b})$ of 7.5 pb, assuming $m_H = 115$ GeV. The limits for four Higgs mass points (105, 115, 125, and 135 GeV) and for ST, DT, and the combined ST+DT results are summarized in Tables II and III. We set 95% C.L. upper limits from 3.4 to 2.5 pb on $\sigma(p\bar{p} \to ZH) \times B(H \to b\bar{b})$ for $m_H = 105$–135 GeV (Fig. 4). The CDF collaboration has published combined limits (ST+DT) with Tevatron Run I data, i.e. at $\sqrt{s} = 1.8$ TeV, of 7.8–7.4 pb for $m_H = 110$–130 GeV [15].

In conclusion, we have performed a search for ZH and WH associated production in the $\not\!\!E_T$+ b jets channel using 260 pb^{-1} of data. We have studied the dijet mass spectrum of the two leading jets with double and exclusive single b-tagged jets for Higgs boson masses between 105 and 135 GeV. In the absence of signal, we have set upper limits on different Higgs production channels/final states, and have combined them. The combined limits are between 3.4 to 2.5 pb (8.3 to 6.3 pb) on the cross section for ZH (WH) production multiplied by the branching fraction for $H \to b\bar{b}$. These are the first limits in the ZH channel based on Tevatron Run II data.

TABLE II: Expected/observed 95% C.L. limits on $\sigma(p\bar{p} \to ZH) \times B(H \to b\bar{b})$ in pb, as a function of m_H.

Higgs mass (GeV)	105	115	125	135
ST	7.7/8.2	6.8/6.8	6.0/7.3	5.4/7.5
DT	3.3/4.2	2.8/3.6	2.5/2.8	2.2/2.2
ST+DT	3.1/3.4	2.7/3.2	2.4/2.9	2.1/2.5

TABLE III: Expected/observed 95% C.L. limits on $\sigma(p\bar{p} \to WH) \times B(H \to b\bar{b})$ in pb, as a function of m_H.

Higgs mass (GeV)	105	115	125	135
ST	18.5/17.6	15.9/16.9	14.9/18.9	12.4/18.5
DT	8.0/9.6	6.6/8.1	6.3/7.1	5.3/5.3
ST+DT	7.6/8.3	6.3/7.5	6.0/7.4	5.0/6.3

We thank the staffs at Fermilab and collaborating institutions, and acknowledge support from the DOE and NSF (USA); CEA and CNRS/IN2P3 (France); FASI, Rosatom and RFBR (Russia); CAPES, CNPq, FAPERJ, FAPESP and FUNDUNESP (Brazil); DAE and DST (India); Colciencias (Colombia); CONACyT (Mexico); KRF and KOSEF (Korea); CONICET and UBACyT (Argentina); FOM (The Netherlands); PPARC (United Kingdom); MSMT (Czech Republic); CRC Program, CFI, NSERC and WestGrid Project (Canada); BMBF and DFG (Germany); SFI (Ireland); The Swedish Research Council (Sweden); Research Corporation; Alexander von Humboldt Foundation; and the Marie Curie Program.

[*] On leave from IEP SAS Kosice, Slovakia.
[†] Visitor from Helsinki Institute of Physics, Helsinki, Finland.

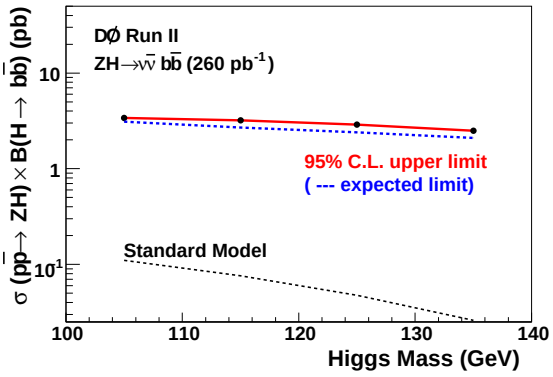

FIG. 4: 95% C.L. upper limit on $\sigma(p\bar{p} \to ZH) \times B(H \to b\bar{b})$ (and corresponding expected limit) for ZH production vs. Higgs mass, as derived from the ST+DT combination.

[1] S. Eidelman *et al.*, Phys. Lett. B **592**, 1 (2004); LEP electroweak working group, http://lepewwg.web.cern.ch/LEPEWWG/
[2] M. Carena *et al.*, hep-ph/0010338.
[3] L. Babukhadia *et al.*, FERMILAB-PUB-03/320-E.
[4] M. L. Ciccolini, S. Dittmaier, M. Kramer, Phys. Rev. D **68**, 073003 (2003).
[5] DØ Collaboration, V. Abazov *et al.*, Phys. Rev. Lett. **94**, 091802 (2005).
[6] CDF Collaboration, A. Abulencia *et al.*, Phys. Rev. Lett. **96**, 081803 (2006).
[7] DØ Collaboration, V. Abazov *et al.*, "The Upgraded DØ Detector," accepted to Nucl. Instrum. Methods Phys. Res. A.
[8] S. Abachi, *et al.*, Nucl. Instrum. Methods Phys. Res. A **338**, 185 (1994).
[9] T. Sjöstrand *et al.*, PYTHIA, Comput. Phys. Commun. **135**, 238 (2001).
[10] M. Mangano *et al.*, ALPGEN, JHEP **0307**, 1 (2003).
[11] A. Pukhov *et al.*, COMPHEP, hep-ph/9908288 (1999).
[12] John Campbell and R.K. Ellis, Phys. Rev. D **65**, 113007 (2002), http://mcfm.fnal.gov/.
[13] R. Brun and F. Carminati, CERN Program Library Long Writeup W5013 (1993).
[14] T. Junk, Nucl. Instrum. Meth. Phys. Res. A **434**, 435 (1999), A. Read in "1^{st} *workshop on Confidence Limits*", CERN report 2000-005 (2000).
[15] CDF Collaboration, D. Acosta *et al.*, Phys. Rev. Lett. **95**, 051801 (2005).